Journal of Catalysis **206,** 40–48 (2002)
doi:10.1006/jcat.2001.3474, available online at http://www.idealibrary.com on IDEAL®

# Nanocrystalline MgO as a Dehydrohalogenation Catalyst

Ilya V. Mishakov,* Alexander F. Bedilo,† Ryan M. Richards,† Vladimir V. Chesnokov,* Alexander M. Volodin,* Vladimir I. Zaikovskii,* Roman A. Buyanov,* and Kenneth J. Klabunde†,[1]

*Boreskov Institute of Catalysis, Novosibirsk 630090, Russia; and †Department of Chemistry, Kansas State University, Manhattan, Kansas 66506

Received May 10, 2001; revised October 31, 2001; accepted November 21, 2001

**Nanocrystalline MgO has been found to be an efficient dehydrohalogenation catalyst. Its reaction with different chlorobutane isomers or 1-bromobutane results in topochemical transformation of the MgO phase to $MgCl_2$ or $MgBr_2$ accompanied by a sharp decrease in the catalyst surface area and increase in its activity. The resulting magnesium chloride and magnesium bromide are very active catalysts for HCl and HBr elimination from halogenated hydrocarbons. The reaction mechanism changes from predominantly E2 elimination on MgO to mostly E1 elimination over $MgCl_2$ and $MgBr_2$, which act as Lewis acids. It was also found that $MgBr_2$ could be completely converted back to MgO by calcination in oxygen at 500°C while $MgCl_2$ oxidation did not occur under similar conditions.** 

*Key Words:* **nanoparticles; MgO; chlorobutane; dehydrohalogenation.**

## INTRODUCTION

The development of novel methods for neutralization of chlorinated wastes has become a very urgent task due to their high toxicity and the significant ecological hazard. Nanocrystalline alkaline earth metal oxides attract significant attention as effective chemisorbents for such toxic gases as $NO_2$, $SO_2$, $SO_3$, and HCl, as well as for chlorinated and phosphorous-containing compounds (1–9). The interaction of such gases with the surface of the nanoparticles is referred to as destructive sorption, as both the surface and the bulk chemical composition of the oxides are often subjected to significant changes during this process. For example, such compounds as $(C_2H_5O)_3P{=}O$ and $(C_2H_5O)_3P$ react with MgO at 500–600°C to give ethylene and solid phosphorous compounds (2). Chloroform reacts with CaO at 300°C as follows (5):

$$4CaO_{(s)} + 2CHCl_{3(g)} \rightarrow 3CaCl_{2(s)} + CaCO_{3(s)} + C_{(s)} + H_2O_{(g)}. \quad [1]$$

$CCl_4$ was found to react with MgO nanoparticles at 500°C according to Reaction [2]:

$$2MgO_{(s)} + CCl_{4(g)} \rightarrow 2MgCl_{2(s)} + CO_{2(g)}. \quad [2]$$

Destructive sorption takes place not only on the surface of oxide materials but also in their bulk. It must be noted that the efficiency of the destructive sorption increases with a decrease in the size of the MgO and CaO crystallites. MgO and CaO work most efficiently in the destructive sorption reaction when their particle size is on a nanometer scale. The high efficiency of the nanoparticle oxides is caused not only by their high surface area but also by the high concentration of low-coordinated sites and structural defects on their surface.

On the other hand, both oxides and salts of alkaline earth metals are known to catalyze dehydrochlorination of chlorinated alkanes (10, 11). With the hope of discovering higher activity catalysts, we have recently been investigating nanocrystalline materials in this type of catalysis. An earlier report dealt with morphological and textural changes that occur when nanocrystalline MgO interacts with 1-chlorobutane (12). Herein we report more detailed studies of the catalytic reactions and attempts to determine the reaction mechanism.

## EXPERIMENTAL

The preparation of starting AP–MgO was described in detail earlier (6). In short, clean pieces of Mg metal were dissolved in methanol under an inert atmosphere to form magnesium methoxide on vigorous stirring for several hours. Deionized water was added dropwise to the$Mg(OCH_3)_2$ solution in a methanol–toluene mixture to form a hydroxide gel, which was dehydrated in an autoclave and heated under dynamic vacuum up to 500°C to yield a nanometer-sized metal oxide.

Dehydrohalogenation reactions were performed in a flow reactor equipped with a McBenn balance, which made it possible to monitor changes in the catalyst weight with $10^{-4}$ g precision. Ultrahigh-purity 99.99% 1-chlorobutane and 99.99% 1-bromobutane were used in these experiments. The halocarbons were introduced into the reactor by saturating the argon flow with $C_4H_9Cl$ or $C_4H_9Br$ vapor

[1] To whom correspondence should be addressed. Fax: (785)-532-6666. E-mail: kenjk@ksu.edu.



0021-9517/02 $35.00

at room temperature. The volume flow rate was 1–2 L/h; the catalyst loading was varied within 0.04–0.08 g. The product composition exiting the reactor was analyzed by an online gas chromatograph. Prior to each experiment MgO was activated in the argon flow at 500°C for 1 h for removal of adsorbed water.

The selectivity to different butene isomers was determined using a Shimadzu GCMS-QP5000 gas chromatograph mass spectrometer equipped with a 30-m Restec capillary column with XTI-5 phase. Samples of the gas flow after the catalyst bed were taken with a gas syringe and injected into the GCMS column. The reactants were 99.5 + % 1-chlorobutane, 99 + % 2-chlorobutane, 98% 1-chloro-2-methylpropane, 99% 2-chloro-2-methylpropane, and 99 + % 1-bromobutane (all from Aldrich), used as received. The volume flow rate for these selectivity experiments was about 30 ml/min; the catalyst loading was 0.04 g. Pulse experiments were performed in the same reactor in order to study changes in the catalyst selectivity at different MgO conversion levels. In this case 10-$\mu$l pulses of the substrate were injected into the saturator. After each injection the gas flow was saturated with the reactant only for a limited amount of time.

The catalysts were studied by transmission electron microscopy TEM using a JEM-2010 microscope (acceleration voltage, 210 kV; spherical aberration coefficient of the object lens, 0.5 mm) with 1.4-Å lattice resolution. X-ray diffraction XRD studies were performed on a Simens D-500 instrument using Cu$K_\alpha$ monochromatic irradiation (graphite monochromator on reflected beam). Silicon powder was used as an internal standard. Lattice parameters were determined from the position of the (200) reflex for MgO and (111) reflex for the $MX_2$ phases. Specific surface area and other textural characteristics of the samples were determined by BET method using thermal desorption of nitrogen.

Thermogravimetric analysis (TGA) was performed on a Shimadzu TGA-50 instrument. The samples were heated in platinum crucibles up to 1000°C with a heating rate of 10°C per min in 30 ml/min ultrahigh-purity helium or dry air flow. The outflow gas mixture was injected once per minute into the GCMS instrument described above through an automatic six-way valve.

## RESULTS AND DISCUSSION

### *Thermodynamic Calculations*

We chose 1-chlorobutane and its homologues 1-bromobutane and 1-iodobutane as model halogenated compounds. The first step consisted of comparative thermodynamic analysis of the feasibility of dehydrohalogenation to 1-butene according to Reaction [3].

$$C_4H_9X \rightarrow C_4H_8 + HX \quad (X = \text{Cl, Br, I}). \qquad [3]$$

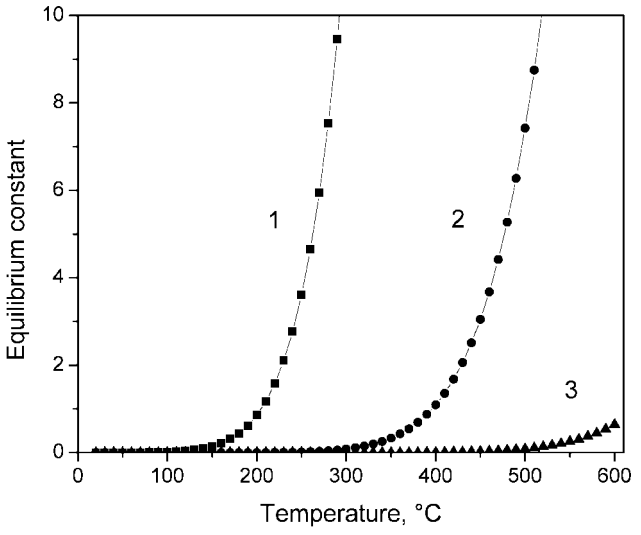


**FIG. 1.** Temperature dependence of the equilibrium constant for dehydrohalogenation of butyl halides to 1-butene: $C_4H_9X \rightarrow C_4H_8 + HX$, where $X$ = Cl (1), Br (2), or I (3).

Then, the temperature dependence of the Gibbs free energy $\Delta G(T)$ was calculated from reference data (13).

$$X = \text{Cl: } \Delta G = 14583 - 30.95\,T + 0.93\ln(T/299),\ \text{cal/mol.}$$
$$X = \text{Br: } \Delta G = 20363 - 31.11\,T + 0.83\ln(T/299),\ \text{cal/mol.}$$
$$X = \text{I: } \Delta G = 27389 - 31.19\,T + 0.64\ln(T/299),\ \text{cal/mol.}$$

Figure 1 presents the temperature dependence of the equilibrium constant for Reaction [3] calculated from the $\Delta G(T)$ equation for the three halocarbons. Judging from these data, 1-chlorobutane should be more susceptible to H$X$ elimination than is 1-bromobutane, while 1-iodobutane should not be subject to it at temperatures below 600°C. Due to these findings, we did not use 1-iodobutane in subsequent experiments.

### *Decomposition of 1-Chlorobutane on AP-MgO*

Figure 2 presents TEM images of the AP–MgO sample. At high magnification one can see that the sample consists of 40- to 60-Å crystallites arranged into chains forming a very porous secondary structure. At lower magnification one can see that the secondary structure is formed by 1.5- to 2-$\mu$m granules. The abundance of pores of different sizes gives AP–MgO a high value of accessible surface area (14).

The possibility of thermal transformations of 1-chlorobutane without a catalyst was studied first. No thermal reactions were observed in an empty reactor in the temperature range of 50–300°C. No more than 1% butylene was observed at 350°C, and the chlorobutane conversion increased to 3% at 400°C.

AP–MgO appeared to have high activity in 1-chlorobutane dehydrochlorination, giving butene and HCl with

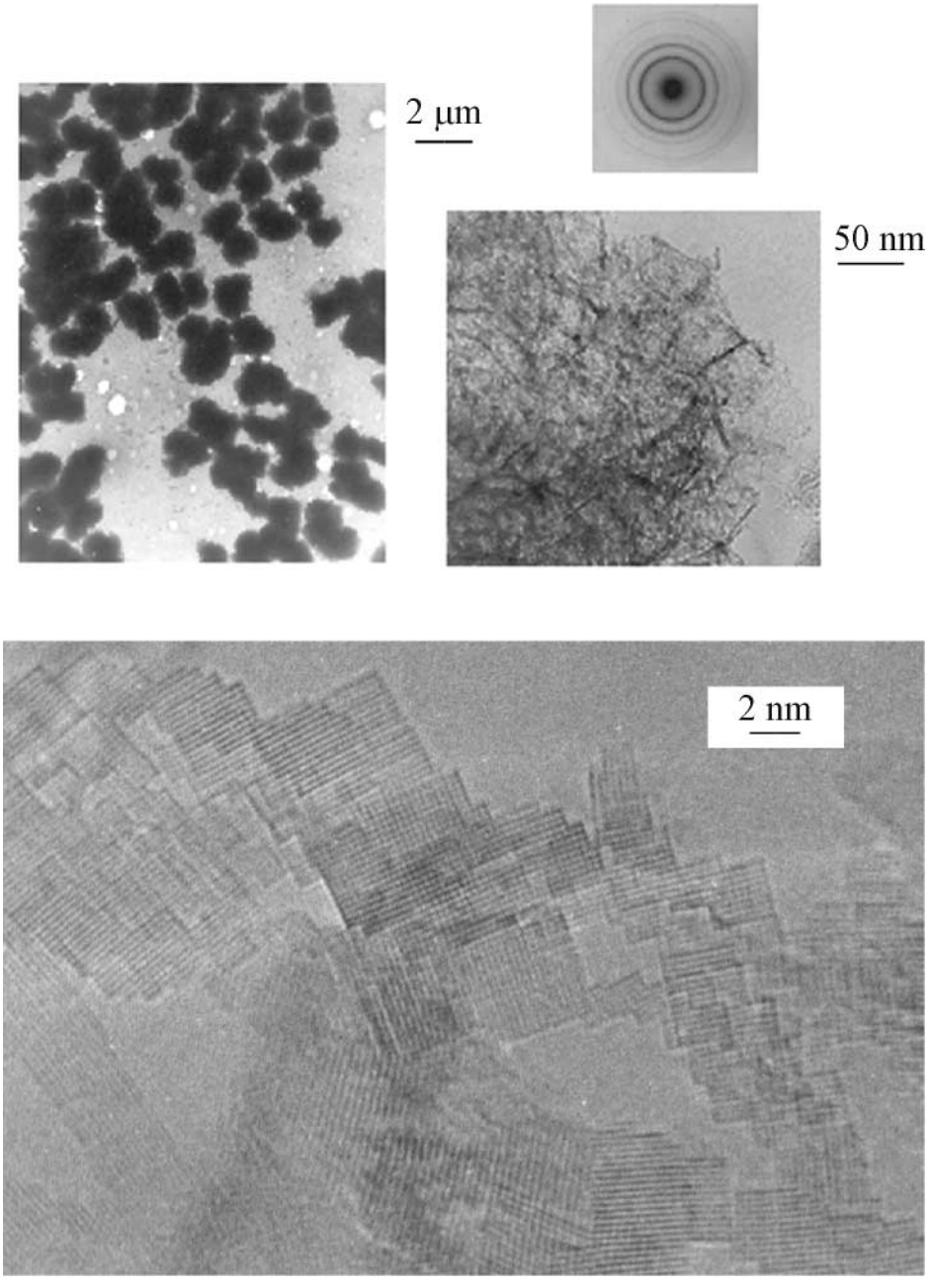


**FIG. 2.** TEM images of initial AP–MgO.

near 100% selectivity. The online chromatograph did not permit us to separate different butene isomers. Such separation was performed in additional experiments employing GCMS analysis of the gas after reactor, which are reported below.

The reaction rate was found to grow by about an order of magnitude during the first hour on stream (Fig. 3, curve 3). It was also found that an increase in catalytic activity was accompanied by growth of the sample weight, indicating a topochemical reaction of MgO chloridation to $MgCl_2$. As the molecular weight of $MgCl_2$ is much higher than that of MgO, this process results in a weight gain (Fig. 3, curve 1). The kinetics of the oxide-to-chloride transformation was also studied at several other temperatures (12). The kinetic weight gain curves have typical S-like shapes at all temperatures studied above 200°C. In the latter case only 8% MgO was transformed to $MgCl_2$ (Fig. 4, curve 1). This seems to indicate that only the surface of the sample was subjected to chloridation while bulk substitution of oxide for chloride does not occur, as the temperature was not high enough.

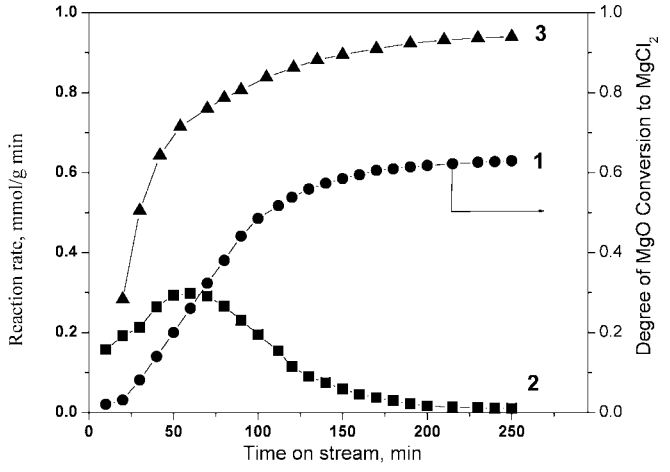


**FIG. 3.** Kinetics of 1-chlorobutane dehydrochlorination over AP–MgO at 350°C: 1, degree of MgO conversion to $MgCl_2$ (right axis); 2, rate of MgO conversion to $MgCl_2$ (left axis); 3, butene formation rate (left axis).

As mentioned above, the appearance of the $MgCl_2$ phase results in a significant increase in catalytic activity. For example, the 1-chlorobutane conversion at 350°C was only 9% after 15 min on stream, while after 1.5 h it was as high as 87%. The textural analysis of the samples after reaction has shown that their surface area actually dropped almost 10-fold. As this was accompanied by conversion enhancement by an order magnitude, this means that the specific catalytic activity of $MgCl_2$ is two orders of magnitude higher that of the initial MgO. So, the solid-state chloridation of MgO to $MgCl_2$ under the action of the reaction medium results in the formation of a very active catalytic system. Hydrogen chloride formed by dehrochlorination of 1-chlorobutane is then partly consumed for further MgO chloridation.

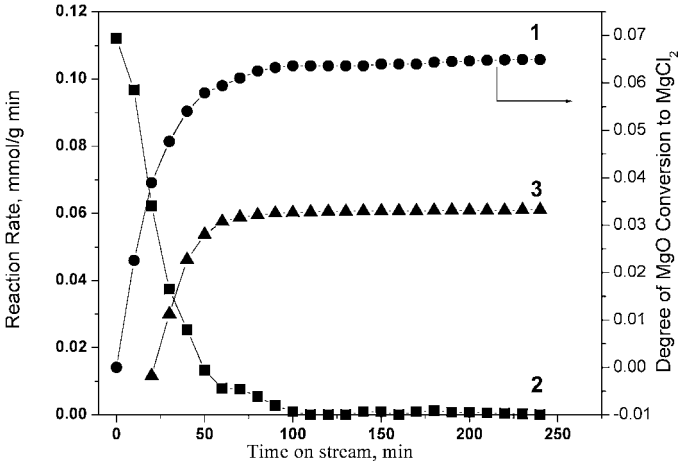


**FIG. 4.** Kinetics of 1-chlorobutane dehydrochlorination over AP–MgO at 200°C: 1, degree of MgO conversion to $MgCl_2$ (right axis); 2, rate of MgO conversion to $MgCl_2$ (left axis); 3, butene formation rate (left axis).

The rates of topochemical transformation of MgO to $MgCl_2$ and 1-chlorobutane dehydrogenation at 350°C are compared in Fig. 3. During the first minutes on stream the rate of the topochemical reaction (curve 2) is almost equal to the butylene formation rate, indicating that almost all HCl detached from 1-chlorobutane is consumed for the MgO chloridation. Then, the rate of the topochemical process gradually grows, reaches a maximum value, and decreases to zero. Such decrease can be explained by the fact that the phase boundary area diminishes as the phase boundary goes inside the nanoparticle aggregates while the $MgCl_2$ crust with low surface area thickens. Continuous thickening of the $MgCl_2$ crust also lowers the diffusion of the reactant to MgO and, thus, reduces the overall rate of the topochemical MgO transformation to $MgCl_2$. This accounts for incomplete transformation of MgO to $MgCl_2$. The butylene formation rate(curve 3) gradually grows and reaches a steady-state value when the topochemical reaction is over, i.e., the catalyst chemical composition does not change any more.

At 200°C the picture is different (Fig. 4). The surface of the oxide is quickly converted to chloride, but the chloridation does not go any further, as indicated by a sharp drop in the topochemical reaction rate (curve 2). The rate of the catalytic reaction quickly reaches a steady-state value and remains constant after that. The conversion of 1-chlorobutane at 200°C is 24%. Note that all reaction rates are much lower at 200 than at 350°C.

An XRD study of the phase composition of the samples after reaction has revealed the presence of three phases—MgO, $MgCl_2$, and $MgCl_2 \cdot 4H_2O$.

The microstructure of the samples after reaction was studied by TEM. The diffraction pattern contained reflections related to both magnesium chloride and magnesium oxide. The catalyst particle aggregates grew slightly in size during the reaction, while their porosity became significantly lower due to the fact that MgO chloridation results in a growth of the phase volume. Unfortunately, no high-quality pictures could be obtained, as this sample proved to be highly hygroscopic.

A detailed analysis of textural transformations taking place in this reaction was reported earlier (12). The pores of the particle aggregates after reaction are filled with magnesium chloride. This makes the surface area of the resulting sample much lower and close to the external surface area of the aggregates. For instance, the surface area dropped from 373 to just 41 $m^2/g$ after 2 h on stream at 350°C (12).

### *Dehydrochlorination of Different $C_4H_9Cl$ Isomers over $MgCl_2/MgO$*

The above experimental data indicate that destructive sorption can account only for the first stage of

1-chlorobutane decomposition on AP–MgO. After the formation of $MgCl_2$ on the surface of the particles, 1-chlorobutane is subjected to catalytic dehydrochlorination. Therefore,the chlorobutane interaction with MgO may be considered as a sum of the heterogeneous catalytic reaction on the surface of the $MgCl_2$/MgO system [4] and the topochemical reaction on the surface and in the bulk of the solid phase [5]:

$$C_4H_9Cl \rightarrow C_4H_8 + HCl, \quad [4]$$

$$MgO + 2HCl \rightarrow MgCl_2 + H_2O. \quad [5]$$

Reaction [4] continues after the termination of Reaction [5]. Correspondingly, HCl formed in Reaction [4] can be either involved in Reaction [5] or removed into the gas phase.

Despite significant decrease in the specific surface area, the catalytic activity of the samples in dehydrochlorination of 1-chlorobutane increases significantly as MgO is converted to $MgCl_2$. The time resolution of the catalytic installation did not allow us to measure the rate of the catalytic reaction on pure MgO, as some $MgCl_2$ was formed even after minimal contact with the feed. Nevertheless, the results obtained bring us to the definite conclusion that the catalytic activity of $MgCl_2$ is significantly higher than that of MgO. This is most likely caused by an increase in the strength of Lewis acid sites on the surface of the catalyst resulting from such transformation as well as from consumption of strong basic sites.

Therefore, it was important to determine if these changes result in any significant changes in the mechanism of the HCl elimination. In contact elimination, as in the liquid phase, it is necessary to distinguish between three main possibilities, as shown in Scheme 1 (11). Here $R_{1-4}$ are hydrogens or alkyl fragments, and $X$ is chlorine or bromine.

The reaction following the E1 mechanism starts with $X^-$ abstraction generating a carbocation, which has a certain lifetime and can be subjected to rearrangement before it loses a proton in the second step. In the case of the E1cB

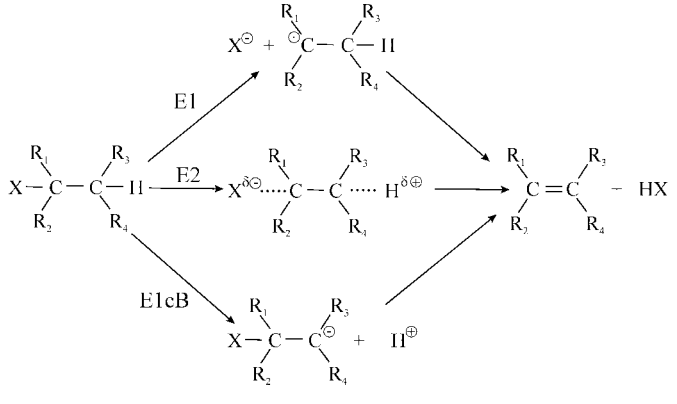


SCHEME 1

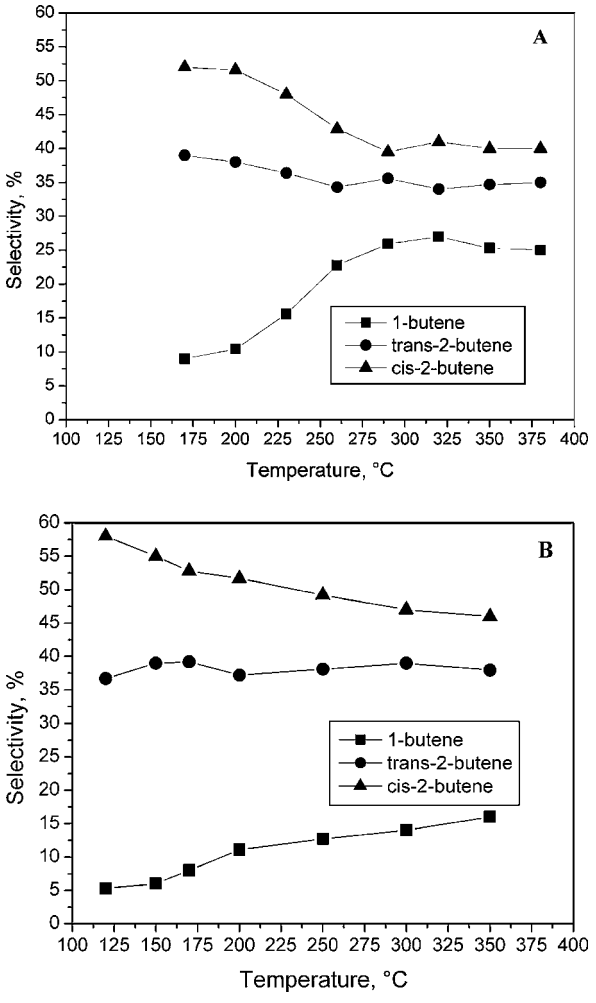


**FIG. 5.** Temperature dependence of the $MgCl_2$/MgO selectivity to different butene isomers during HCl elimination from 1-chlorobutane (A) and 2-chlorobutane (B).

mechanism the reaction also consists of two distinct steps, beginning with the proton abstraction. The E2 mechanism covers a broad range between the two, with $H^+$ and $X^-$ removed simultaneously in a concerted process. Its essential feature is that the energy process has only one maximum.

If no rearrangement of the carbocation takes place, 1-butene should be the only product resulting from the dehydrochlorination of 1-chlorobutane. Initial experiments involving separation of the butene isomers showed that this was not the case, as significant amounts of *trans*- and *cis*-2-butenes were formed (Fig. 5). The graph shows the selectivity of the same catalyst in a steady state, when its surface had been already converted to $MgCl_2$. Note that the distributions of products formed from 1-chlorobutane and 2-chlorobutane are very similar, especially at low temperatures (<250°C).

The formation of 2-butene isomers as predominant products in the reaction of 1-chlorobutane appears to indicate that the HCl elimination follows the E1 mechanism. The

reaction starts with $Cl^-$ abstraction by a surface Lewis acid site. The resulting primary carbocation is then rearranged to a much more stable secondary cation that is eventually subjected to deprotonation to form a mixture of 1-butene, *trans*-2-butene, and *cis*-2-butene. At low temperatures the isomers are formed in the exact same amounts as in the case of 2-chlorobutane, where the secondary carbocation is formed directly by $Cl^-$ abstraction. Higher selectivity to 1-butene at temperatures above 250°C is either due to a contribution of the concerted mechanism or due to a shortening of the cation lifetime when some of the cations are not subjected to rearrangement before deprotonation.

These results are in good agreement with the earlier observation that Mg salts usually act as pronounced E1 catalysts in contact elimination reactions (11). Another notable feature is the fact that the amount of *cis*-2-butene always exceeds that of a more thermodynamically stable *trans*-isomer. However, such behavior is often observed in contact eliminations (11, 15). It seems quite natural that the formation of *cis*-olefins on a catalyst surface should be preferred for steric reasons.

In order to determine if the mechanism is different on the initial MgO, we performed an experiment in which we injected small amounts of 1-chlorobutane into the saturator (Fig. 6). In this case, the total of five injections was approximately equal to the amount of 1-chlorobutane necessary to convert all MgO to $MgCl_2$ provided that all hydrochloric acid eliminated from 1-chlorobutane was used for the reaction with MgO. One can see that the 1-chlorobutane of the first injection is converted primarily to 1-butene. This indicates that MgO initiates the E2 elimination due to the presence of strong basic sites on its surface, together with relatively weak Lewis acid sites. Then, the 1-butene selectivity goes down to the steady-state value as the MgO surface is being converted to $MgCl_2$. Meanwhile, the 1-butene selectivity in the reaction of AP–MgO with 2-chlorobutane did not depend on the MgO conversion degree (Fig. 6).

Table 1 summarizes the performance of partially chlorinated MgO as a catalyst for HCl elimination from different chlorobutane isomers. These data were deliberately obtained on one sample, which was initially prepared by a 2-h reaction of AP–MgO with 1-chlorobutane at 300°C. The resulting material apparently was not subjected to any significant sintering or coking during subsequent experiments with different isomers performed at lower temperatures, as both its activity and selectivity were very stable and could be readily reproduced several times within a reasonably small error.

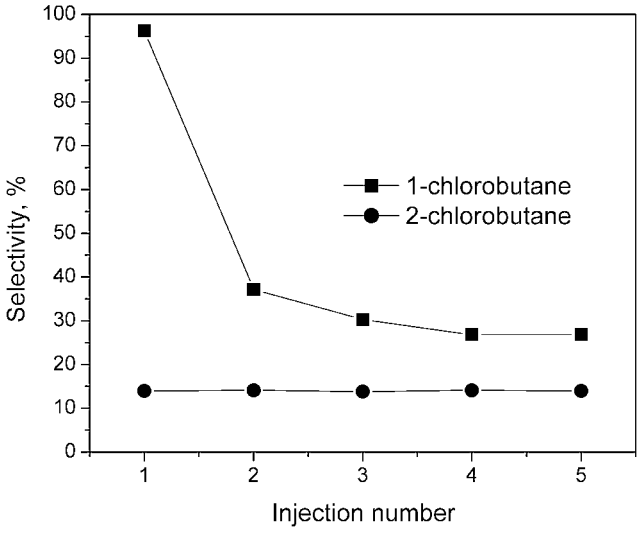


**FIG. 6.** Changes in the 1-butene selectivity of AP–MgO at 300°C with the amount of substrate passed through the catalyst bed.

The following order of reactivity was observed for the chlorobutane isomers over $MgCl_2$/MgO, as evidenced by both the lowest temperatures with 5 + % conversion and conversions at 200°C:

$$\text{1-chlorobutane} < \text{1-chloro-2-methylpropane} < \text{2-chlorobutane} < \text{2-chloro-2-methylpropane}.$$

This order matches the well-known order for the ease of chloride removal. This appears to indicate that chloride abstraction by a Lewis acid site is the rate-determining step in the reaction following the E1 mechanism. Notably, thermodynamic calculations similar to the ones reported above with data for chlorobutane isomers taken from Ref. (13) give us a completely different order (Fig. 7). Obviously, this means that no true equilibrium of Reaction [3] is achieved, while chloride and proton are removed in two separate steps. This makes it possible to achieve conversions at low

**TABLE 1**

**Dehydrochlorination of Chlorobutane Isomers over $MgCl_2$/MgO**

| Compound | Lowest temperature with 5+% conversion (°C) | Conversion at 200°C (%) | Selectivity at 200°C (%) | | | | Activation energy, kJ/mol | Temperature range (°C) |
|---|---|---|---|---|---|---|---|---|
| | | | Isobutene | 1-Butene | *trans*-2-butene | *cis*-2-butene | | |
| 1-Chlorobutane | 170 | 32 | 0 | 10 | 38 | 52 | 99 | 170–250 |
| 2-Chlorobutane | 120 | 93 | 0 | 11 | 37 | 52 | 95 | 120–200 |
| 1-Chloro-2-methylpropane | 150 | 40 | 87 | 1 | 6 | 6 | 70 | 150–230 |
| 2-Chloro-2-methylpropane | 60 | 97 | 99 | 0 | 0 | 1 | 50 | 50–150 |

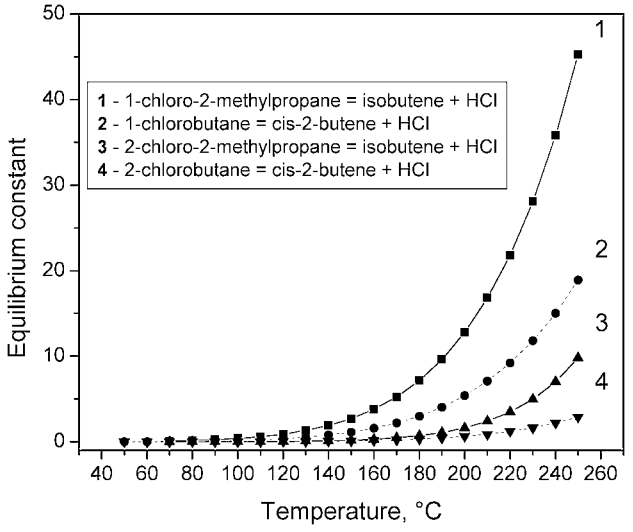


**FIG. 7.** Temperature dependence of the equilibrium constant for dehydrohalogenation of chlorobutane isomers to the major products formed from them.

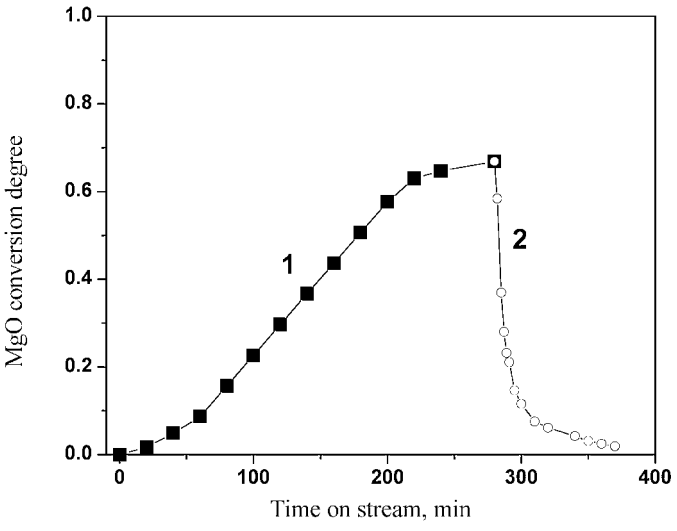


**FIG. 8.** Degree of AP–MgO conversion to $MgBr_2$ vs time on stream: 1, $C_4H_9Br$ dehydrobromination at 400°C; 2, regeneration in $O_2$ at 500°C.

temperatures well above those predicted by the thermodynamics.

*Dehydrobromination of 1-Bromobutane over AP–MgO*

Similar experiments were performed using 1-bromobutane as a substrate. The butylene selectivity in this case was also close to 100%. The main features of this process appeared to be very similar to those described above for 1-chlorobutane. The only major exception was the lower catalytic activity of $MgBr_2$ formed as a result of the topochemical reaction. Complete MgO conversion to $MgBr_2$ was also not achieved during the 1-bromobutane dehydrobromination (Fig. 8).

The distribution of products formed from 1-bromobutane was very similar to that observed in the case of 1-chlorobutane (Fig. 9). Again, 1-butene is a predominant product in the first moments of the reaction. Later, as the MgO surface is partially converted to $MgBr_2$, significant amounts of 2-butenes start forming. These data indicate that in the case of 1-bromobutane MgO also acts as an E2 elimination catalyst, while the bromide formed is a more active E1 catalyst.

As the sample was black after reaction, it was initially supposed that this was due to the formation of a surface carbon layer. Therefore, we attempted to regenerate the sample after it reached a stable weight, indicating termination of MgO bromidation, in order to determine the bromidation degree. It was found that it was possible not only to clear the catalyst surface by calcination in oxygen at 500°C but also to convert all $MgBr_2$ back to MgO (Fig. 8).

Figure 10 presents the results of the TGA analysis of samples after reaction. The samples were collected after 2 h on stream. The reaction temperature was 300°C for 1-chlorobutane and 350°C for 1-bromobutane. Curves 1 and 2 were obtained for the same sample under the flow of air and ultrahigh-purity helium. Trace amounts of oxygen present in the second case are still sufficient for complete oxidation of the sample, but this happens at much higher temperature than in the case of air.

The results of the TGA–GCMS analysis of the flow leaving the sample are shown in Fig. 11. The three peaks observed in the spectrum of water (curve 2) match well with the weight loss peaks at 155, 220, and 345°C present in the derivative TGA spectrum (curve 1). The total weight loss in the temperature range below 360°C corresponding mostly to water in different states is about 14%. As this water is

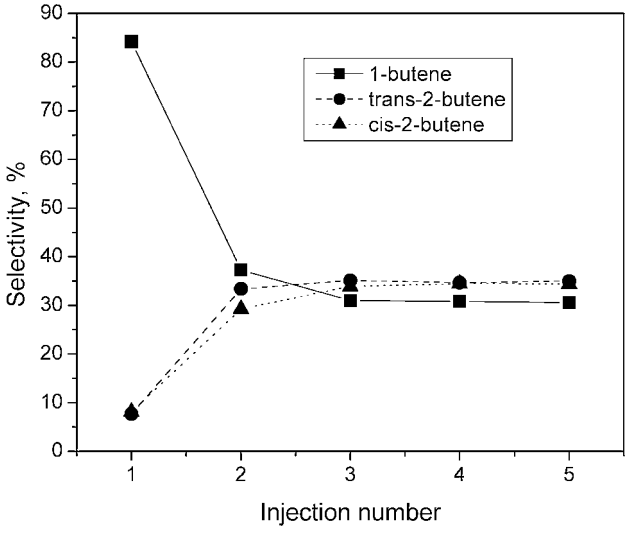


**FIG. 9.** Changes in the selectivity of AP–MgO during the reaction with 1-bromobutane at 350°C with the amount of substrate passed through the catalyst bed.

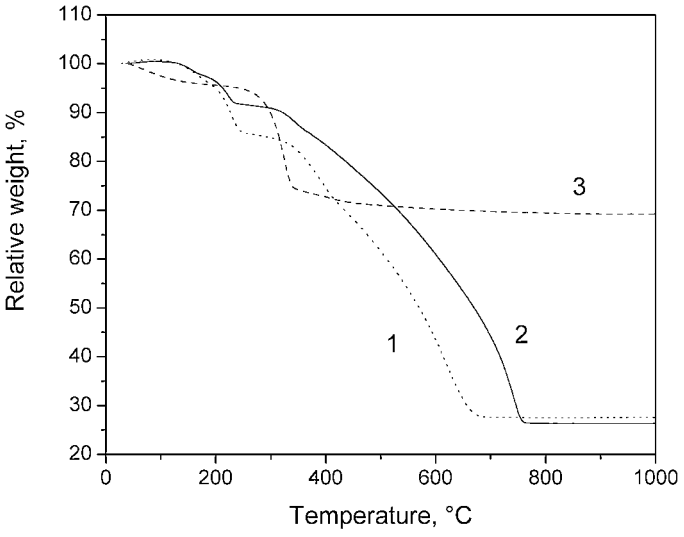


**FIG. 10.** TGA profiles of AP–MgO samples after a 2-h reaction with 1-bromobutane at 350°C (1, 2) and 1-chlorobutane (3). TGA flow gases are dry air (1) and high-purity helium (2, 3).

mostly lost at temperatures below the reaction temperature, no water is expected to be present in the sample during the reaction. It seems to originate from absorption during the sample transfer from the reactor to the TGA chamber.

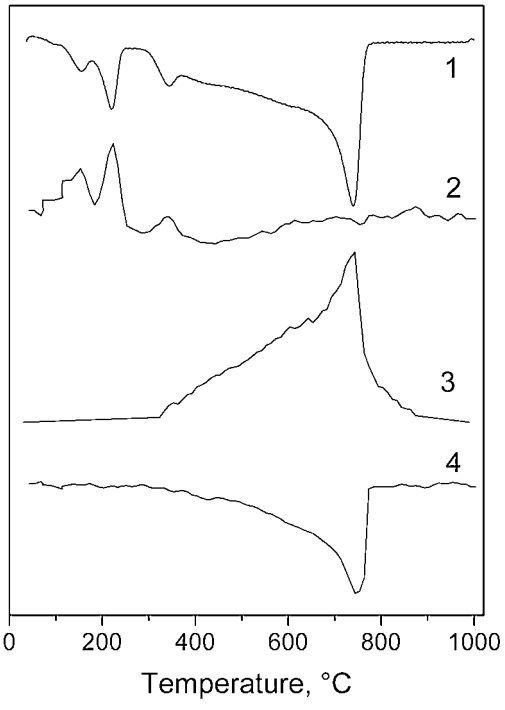


**FIG. 11.** Derivative TGA profile of the sample after reaction with 1-bromobutane at 350°C (1). and MS profiles of water ($m/z = 18$, curve 2), HBr ($m/z = 80$, curve 3), and $O_2$ ($m/z = 32$, curve 4). Derivative TGA peaks going down correspond to more intense weight loss. MS peaks going up represent higher amounts of the corresponding species in the flow. All intensities are arbitrary.

HBr is the main product corresponding to the large weight loss peak at 740°C (curve 3). Note a matching decrease in the concentration of oxygen in the flow (curve 4). This seems to indicate that the first step of this process is $MgBr_2$ reaction with oxygen to form MgO. Bromine released in this process appears to react with water present in the furnace to give HBr. No molecular bromine was observed at the detector.

Although the black color of the sample after reaction undoubtedly indicates coke formation on the surface, the amount of $CO_2$ formed during the TGA run was relatively small. So, most of the weight loss at temperatures above 360°C corresponds to the $MgBr_2$ conversion to MgO. The total weight loss in this range exceeded the final weight of the sample after the TGA experiment by a factor of 2.2, which corresponds to 55% MgO conversion to $MgBr_2$ during the reaction with 1-bromobutane.

Note that no $MgCl_2$ oxidation occurred under similar conditions in the case of the sample obtained after the MgO reaction with 1-chlorobutane (Fig. 9, curve 3). Water was the only product detected by GCMS during the only significant weight loss (about 25%) of this sample observed around 325°C. No HCl or other chlorine-containing molecules were detected. A larger amount of water formed in this case in comparison with the bromidated sample is in good agreement with the phenomenological observation that $MgCl_2$ is more sensitive to water than is $MgBr_2$. The nearly white color of the sample after reaction and an almost negligible amount of $CO_2$ released during the TGA experiment indicate that practically no coking takes place during reaction with 1-chlorobutane at 300°C.

## CONCLUSIONS

Nanocrystalline MgO has been found to react with chloro- or bromobutane to form an outer layer of $MgCl_2$ or $MgBr_2$, respectively. These $MgX_2$ layers possess very active sites for subsequent catalytic dehydrohalogenation of the halocarbons to a mixture of butene isomers mainly by an E1 mechanism.

## ACKNOWLEDGMENT

This study was supported by the Russian Foundation for Basic Research (Grant 00-15-97440) and the U.S. Army Research Office.

## REFERENCES

1. Li, Y.-X., and Klabunde, K. J., *Langmuir* **7**, 1388 (1991).
2. Li, Y.-X., Koper, O. B., Atteya, M., and Klabunde, K. J., *Chem. Mater.* **4**, 323 (1992).
3. Koper, O. B., Lagadic, J., Volodin, A. M., and Klabunde, K. J., *Chem. Mater.* **9**, 2468 (1997).
4. Koper, O. B., Lagadic, J., and Klabunde, K. J., *Chem. Mater.* **9**, 838 (1997).

5. Koper, O. B., and Klabunde, K. J., *Chem. Mater.* **9**, 2481 (1997).
6. Klabunde, K. J., Stark, J. V., Koper, O. B., Mohs, C., Park, D. G., Decker, S., Jiang, Y., Lagadic, J., and Zhang, D., *J. Phys. Chem.* **100**, 12142 (1996).
7. Koper, O. B., Li, Y.-X., and Klabunde, K. J., *Chem. Mater.* **5**, 500 (1993).
8. Jiang, Y., Decker, S., Mohs, C., and Klabunde, K. J., *J. Catal.* **180**, 24 (1998).
9. Itoh, H., Utamapanya, S., Stark, J. V., Klabunde, K. J., and Schlup, J. R., *Chem. Mater.* **5**, 71 (1993).
10. Noller, H., and Kladnig, W., *Catal. Rev.–Sci Eng.* **13**, 149 (1976).
11. Noller, H., Andreu, P., and Hunger, M., *Angew. Chem. Int. Ed.* **10**, 172 (1971).
12. Fenelonov, V. B., Mel'gunov, M. S., Mishakov, I. V., Richards, R. M., Chesnokov, V. V., Volodin, A. M., and Klabunde, K. J., *J. Phys. Chem. B* **105**, 3937 (2001).
13. Treger, Yu. A., "Reference Book on Physicochemical Properties of C1-C5 Chlorinated Aliphatic Compounds" (in Russian). Khimiya, Moscow, 1973.
14. Richards, R., Li, W., Decker, S., Davidson, C., Koper, O., Zaikovskii, V., Volodin, A., Rieker, T., and Klabunde, K. J., *J. Am. Chem. Soc.* **122**, 4921 (2000).
15. Knozinger, H., and Buhl, H., *Z. Phys. Chem.* **63**, 199 (1969).